Neutral dissociation of superexcited states in nitric oxide

ARTICLE *in* CHEMICAL PHYSICS · AUGUST 2003

Impact Factor: 1.65 · DOI: 10.1016/S0301-0104(03)00296-9

Available online at www.sciencedirect.com
SCIENCE DIRECT®
Chemical Physics 293 (2003) 65–73
Chemical Physics
www.elsevier.com/locate/chemphys

Neutral dissociation of superexcited states in nitric oxide

E. Melero García[a,*], J. Álvarez Ruiz[a], P. Erman[a], A. Kivimäki[a], E. Rachlew-Källne[a], J. Rius i Riu[a], M. Stankiewicz[a,b], L. Veseth[c]

[a] Section of Atomic and Molecular Physics, The Royal Institute of Technology, AlbaNova, SE-106 91 Stockholm, Sweden
[b] Instytut Fizyki im. Mariana Smoluchowskiego, Jagellonian University Reymonta 4, 30-059 Kraków, Poland
[c] Department of Physics, University of Oslo, N0316 Oslo, Norway

Abstract

Near-infrared dispersed fluorescence measurements of 13 different atomic multiplets of neutral atomic fragments from photon induced neutral dissociation processes in NO are reported. For excitation of the molecules narrow band synchrotron photons of energy 17.2–25.8 eV were used. Neither Rydberg series nor other molecular states in NO known so far can account for the collected data. From ab initio calculations we try to obtain more information regarding the NO precursor states, and the mechanism behind the observed neutral dissociation.

1. Introduction

Superexcited states, i.e., excited states of molecules above the first ionization limit, play a key role in the dynamics of molecular systems after photon absorption. A superexcited state is an intrinsically unstable system that can release its excess of energy in several ways the most common ones being autoionization and fragmentation into neutral fragments (neutral dissociation ND) that can be in an excited state themselves. In the latter case the process can be studied by means of fluorescence spectroscopy of the radiative decay of the fragments. Knowledge about the fragmentation dynamics of these states is an important piece of information, for example, for tracking photon induced chemical reactions occurring in the upper layers of the atmosphere. For this reason a significant amount of research has been carried out in gaseous molecules that are abundant in the atmosphere. For ND studies there are fairly recent publications in CO [1–3], N_2 [4,5], O_2 [6,7] and NO [8,9] observing the fluorescence of the atomic fragments in the VUV [1,2,4,6,8,9] and the visible region [3,5,7,8]. By measuring the fluorescence of the atomic fragments it is possible to determine the symmetries of the excited states of the atoms. Since the electric dipole rules constrain the possible symmetries to be reached from a specific symmetry of the ground state, ab initio calculations may reveal the states responsible for the neutral dissociation process. This was the goal of the studies in CO [3], N_2 [5] and O_2 [7]. In the case of CO [4] groups of valence states of $^1\Pi$, $^3\Sigma^-$ and $^3\Sigma^+$ seemed to be the precursor states for the dissociation

* Corresponding author. Tel.: +46-8-5537-8114; fax: +46-8-5537-8601.
E-mail address: emilio@atom.kth.se (E. Melero García).

0301-0104/$ - see front matter © 2003 Elsevier Science B.V. All rights reserved.
doi:10.1016/S0301-0104(03)00296-9

channels studied. For N_2 it was concluded that the mediating states were a number of non-Rydberg doubly excited resonances (NRDERs), a 'new family' of molecular states previously observed in [10], and a set of valence states of triple symmetry were found to be responsible for the dissociation in O_2 [7]. The NO studies performed in [8] with undispersed fluorescence in the visible (300–650 nm) and VUV region (110–200 nm) registered VUV emission from OI ($3s^3S^0$) and NI ($3s^4P$) fragments with thresholds of 16.02 and 16.82 eV, respectively. In [8], the predissociation of Rydberg states of NO is pointed out as the responsible process for these atomic emissions. In [9], dispersed VUV emission of excited NI ($3s^2P$) fragments is recorded and displayed as a function of exciting energy. Again, predissociation of neutral Rydberg series is suggested to be the origin of the production of the neutral excited N atoms. The aim of the present work is to gain deeper knowledge of the dissociation mechanism by measuring dispersed fluorescence in the near infrared region of NO, which allows us to investigate higher lying states that would then be populating the lower levels studied in [8,9], thus giving us a deeper insight in the process of the fragmentation of the molecule.

2. Experiments and results

The experiments were performed at the beam line 52 of the MAX I storage ring at the Swedish national synchrotron facility MAX, in Lund. This beam line has a bending magnet as source of photons that are monochromatized by a 1 m normal incidence monochromator (NIM). The slits of the NIM were set to 300 μm thus giving a resolution of 65 meV at $h\nu = 20$ eV.

Our experimental chamber, along with recent modifications, will be described in a forthcoming publication. Briefly, it consists of a vacuum chamber connected to a differential pumping stage by a capillary with 2 mm inner diameter, allowing synchrotron light to be transmitted through, while keeping the ambient pressure low enough to match the requirements of the beam line. The gas inlet system for the NO molecules consisted of a three directional manipulator with a nozzle attached, that allows working with a pressure approximately two orders of magnitude higher in the interaction region than in the rest of the chamber. Tests on the influence of pressure on the acquired signal were accomplished, resulting in a compromise at 5×10^{-3} mbar. Above this value absorption started to reduce the light emission. Fluorescence during de-excitation was collected perpendicularly to the synchrotron beam by a spherical mirror and sent through a glass window. A lens outside the chamber focused the emitted light onto the entrance slit of a 0.46 m focal length spectrometer, equipped with a 600 l/mm grating (Jobin–Yvon HR460). Dispersed photons were recorded using a liquid nitrogen cooled CCD detector that ensures a low dark count level.

In Fig. 1 a small section of a typical spectra from our instrument acquired at 21.37 eV exciting photon energy is shown. This section includes the partially resolved NI 3s $^4P \rightarrow 3p\ ^4P^0$ multiplet and minute contributions from NI $3s'\ ^2D \rightarrow 5p\ ^2D^0$. In total we studied 13 distinct multiplets, 10 corresponding to levels of NI and 3 of OI. A scheme of these levels is shown in Fig. 2 together with possible NO precursor states that are known to exist in this region, i.e., the NO Rydberg series R(A) and R(c) converging to the A and c states of NO^+, respectively. The multiplets were integrated separately and their intensities plotted versus the ex-

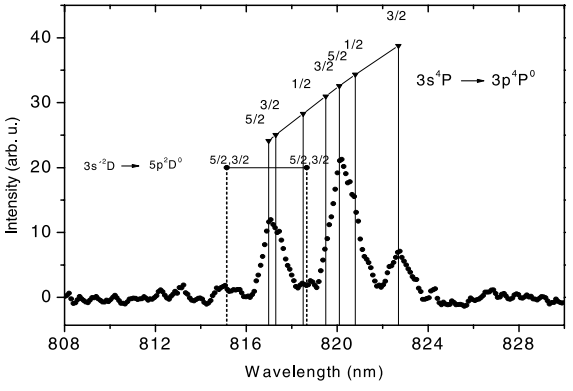

Fig. 1. The multiplet 3s $^4P \rightarrow 3p\ ^4P^0$ of neutral nitrogen formed in neutral dissociation of nitric oxide following excitation by 21.37 eV photons. This spectrum forms a unique fingerprint of this multiplet and contributions from the close lying multiplet $3s'\ ^2D \rightarrow 5p\ ^2D^0$ are negligible.

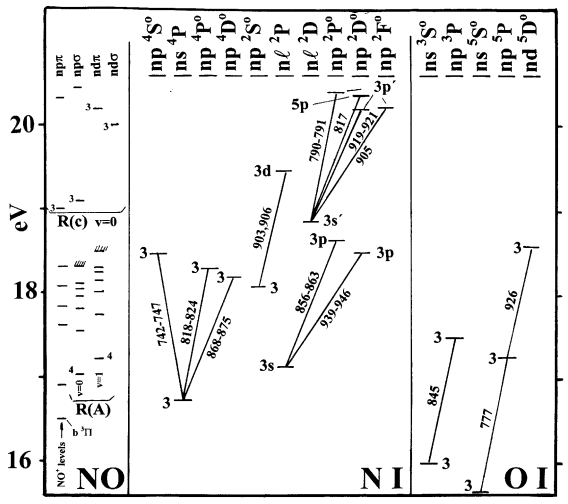

Fig. 2. Partial level diagram of multiplets in neutral nitrogen and oxygen observed in the present work following neutral dissociation of photon excited nitric oxide. The energies of the levels are relative to the ground state of NO assuming that the dissociations have the limits N* + O (g.s.) or N (g.s.) + O*. To the far left are given for comparison the energy levels in NO^+ from b $^3\Pi$ up to A $^1\Pi$. The Rydberg series *R*(A) and *R*(c) converging to the A and the c state of NO^+, respectively, are also indicated.

citing photon energy. The excitation functions obtained in this way are displayed in Fig. 3, where the experimental points are connected as a guide to the eye. The position of the Rydberg *R*(A) and *R*(c) levels are also included. The vertical arrows in Figs. 3(a)–(d) indicate the calculated thresholds for exciting the actual multiplet. It follows that in the majority of the studied cases the observed emission starts already at the threshold, which indicates that the dissociating state is attractive. The excitation functions for the NI quartets (Fig. 3(a)) and the doublets from 3p, $^2P^0$ and $^2D^0$ (Fig. 3(b)), all have a peak in the 18–19 eV excitation region. This region is above the *R*(A) levels and below the *R*(c) levels and it is unlikely that these Rydbergs levels can be the precursors of the observed neutral dissociations into N* + O (g.s.).

All the NI excitation functions in Figs. 3(a)–(c) show in addition at least two peaks in the 20–22 eV region. It is unlikely that the *R*(c) levels could be the precursors for most of the emission since higher Rydberg levels should be only weakly populated.

Concerning the neutral dissociation into N (g.s.) + O*, the observed peaks in the excitations functions (Fig. 3(d)) also poorly coincide with the known Rydberg levels. Accordingly ab initio computations are needed to trace the "new" NO states which cause the studied neutral fragmentation processes of NO.

3. Ab initio calculations

To better understand the mechanisms behind the observed neutral dissociations in NO we have carried out ab initio calculations for the relevant range of excitation energies. With its open-shell ground state NO yields a large amount of excited configurations, with a subsequent large and complicated set of excited states of various symmetries. Thus, in our ab initio study we have limited ourselves to doublet states that can be reached from the $^2\Pi$ ground state via electric dipole transitions, and which might be molecular precursor states for the observed dissociation processes. Furthermore, we have also restricted our analysis to the doublet states that correlate with the observed atomic dissociation products, expecting these to be the relevant precursor states.

Our present ab initio method is basically a rather straightforward CI calculation, however, based on the Kohn–Sham (KS) orbitals of density functional theory (see [11,12] and references given therein). KS orbitals based on exact local exchange potentials have the favourable feature that unoccupied excited orbitals rather closely describe real excited ones, in contrast to, e.g., the unphysical virtual orbitals of Hartree–Fock theory [13,14]. Consequently, rather short CI-expansions based on KS-orbitals have been found to yield accurate excitation energies [12], with corresponding excited configurations that are also physically meaningful.

In the present investigation KS orbitals were obtained by use of an extended set of Slater atomic orbitals. A total of 26 orbitals of σ-symmetry were included, as well as 18 of π-symmetry, and 8 of δ-symmetry. The optimised basis set of Cade and Wahl [15] was extended by several diffuse 3s, 4s, 3p, 4p and 3d orbitals to account for Rydberg character of the excited orbitals. The molecular

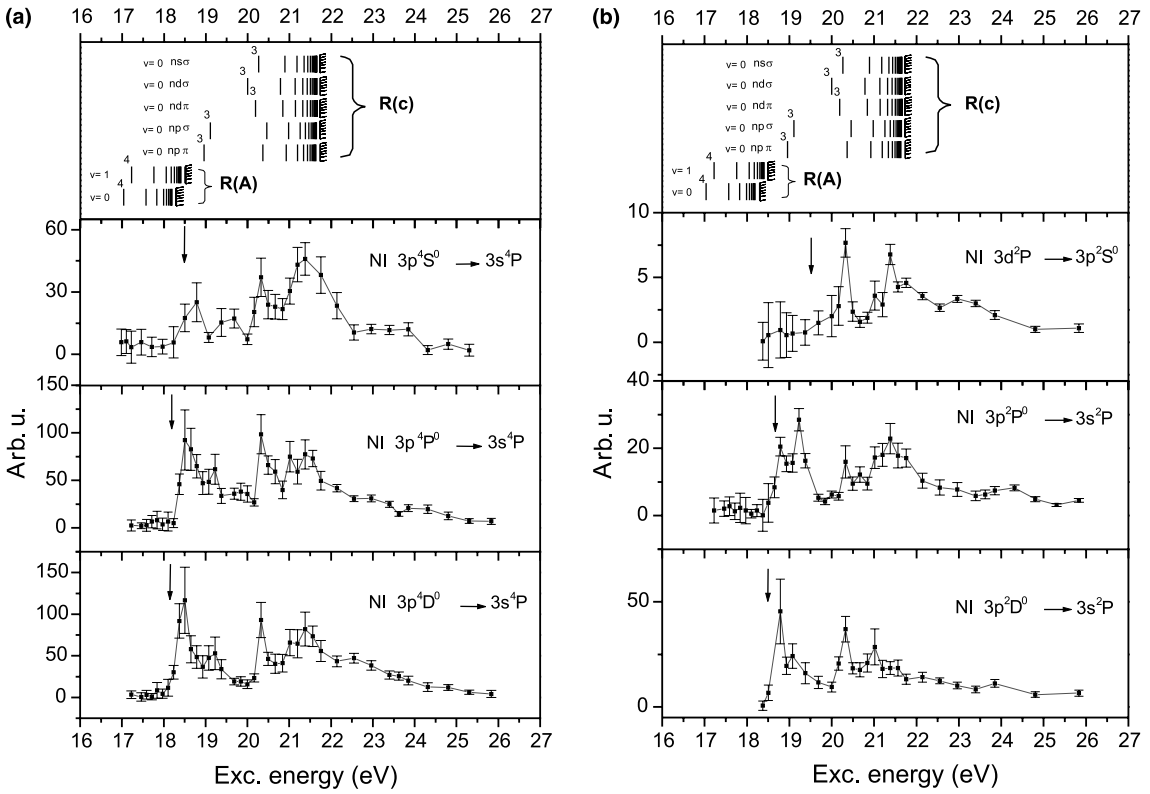

Fig. 3. Measured excitation functions of atomic multiplets in neutral nitrogen and oxygen formed by neutral dissociation of nitric oxide excited by 17.2–25.8 eV photons. On the top of each figure the positions of experimentally known NO Rydberg levels in the actual excitation region are indicated. The vertical arrows locate the thresholds for exciting the multiplet. The continuous lines joining the measured points just serve as a guideline to the eye.

states that correlate with a specific atomic dissociation product were worked out by use of the Wigner–Witmer rules [16]. In this process we had to start from the very lowest ground state dissociation limit, identifying and counting all molecular states of a given symmetry up to our specific limit. In this way we found that there are, e.g., two states of $^2\Pi$ symmetry correlating with the $N3p^4P + O^3P$ (g.s.) limit, and that these two states are numbers 28 and 29 counting upwards from the $^2\Pi$ ground state. In the present CI-expansion 85 Π-symmetry configurations were included, yielding a total of 253 $^2\Pi$ states. Similar numbers apply to states of other symmetries. Thus, we expect that all $^2\Pi$ states in the relevant energy region are accounted for, including numbers 28 and 29 mentioned above.

4. Computed results and comparison with experiment

Table 1 shows some selected computed results from the present CI expansion. To give a full account of all the states terminating at all the present observed dissociation limits would be a rather unwieldy task, so we have concentrated on just the four low-lying limits included in the table. Table 1 gives computed vertical excitation energies at the NO $^2\Pi$ ground state equilibrium internuclear separation $R_e = 2.1747$ a.u. Electric dipole strengths are also computed and included, defined by the relation

$$|\vec{r}_{fi}|^2 = \frac{1}{3}\left[|\langle f|x|i\rangle|^2 + |\langle f|y|i\rangle|^2 + |\langle f|z|i\rangle|^2\right], \qquad (1)$$

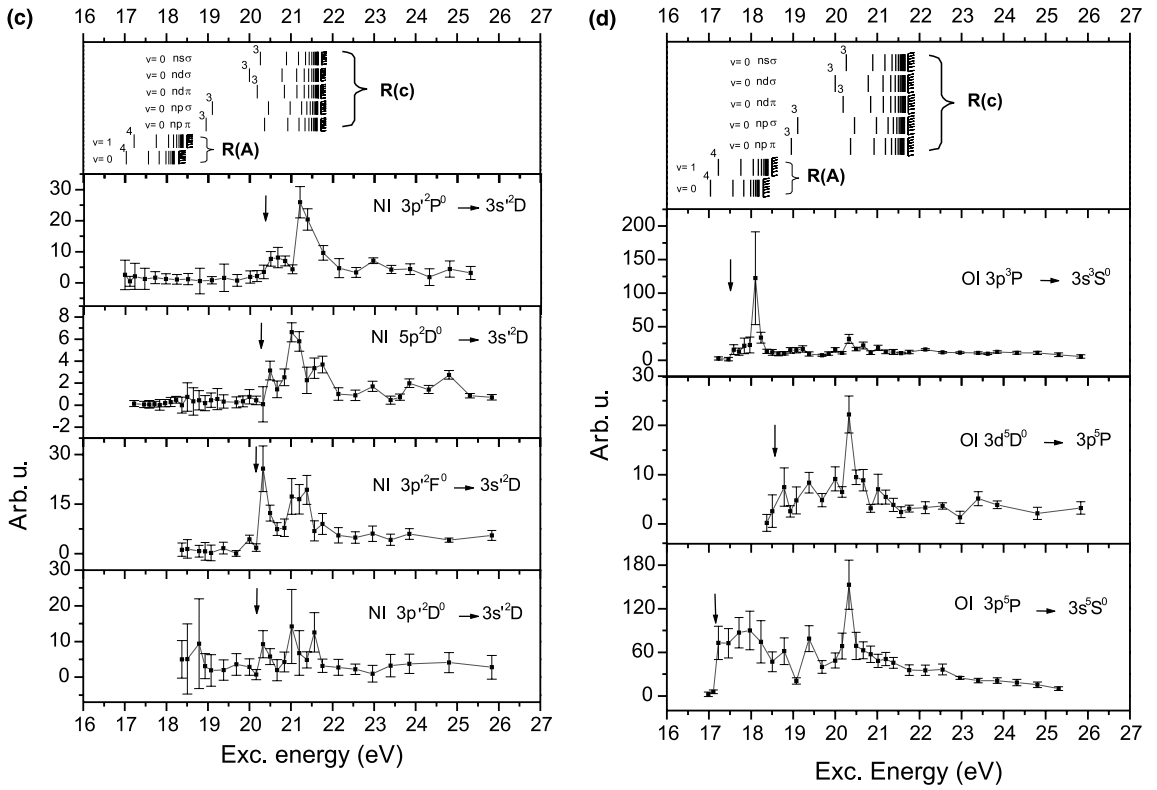

Fig. 3. (*continued*)

where f and i represent final and initial states, respectively. The electric dipole strengths are seen to vary by orders of magnitude between different states, and they are also subject to large and irregular variations with the internuclear separation due to avoided crossings among the respective excited state potential curves. The excited states from Table 1 are in most cases ascribed to the interaction between two dominant configurations. All the involved excited orbitals are bound, i.e., with negative orbital energies. In the Hartree–Fock description they would all (except the 3π orbital) have positive energies, and the excited states would be ascribed to more extensive mixtures of unphysical configurations. We also notice that except for the single and double excitations to the 2π orbital, all listed excitations are to states of Rydberg character.

Figs. 4–6 show potential curves for doublet states expected to terminate at the selected dissociation limits. Unfortunately, numerical problems prohibited the extension of the potential curves to R-values above 2.70 a.u. A typical feature of all the potential curves displayed is that they seem to tend to dissociation limits well above the expected ones. This situation prevails even with reasonable allowance for inaccuracies in the computed excitation energies. However, several of the highest curves tend to flatten or even make a down turn at the highest R-values. This indicates that the curves have potential maxima at some higher R-value. A reason for such maxima might be that they are basically of Rydberg character (cf. Table 1), and in a diabatic manner they actually tend to dissociation limits (far) above the current non-Rydberg atomic levels. The computed curves are, however, adiabatic curves, which through avoided crossings will be turned down to the expected limits.

All the potential curves shown in Figs. 4–6 represent bound states that may hold several

Table 1
Computed vertical excitation energies and electric dipole strengths (Eq. (1)) for molecular doublet states that correlate with the indicated atomic dissociation limits

Atomic and molecular states	Vertical ex. energy (eV) $R = 2.1747$ a.u.	El. dipole strength (a.u.)	Dominant excitation
N $3p^4P^0$ + O ^3P			
$^2\Pi$	18.21	0.00025	$1\pi \rightarrow 5\pi$ (R)
$^2\Pi$	18.15	0.0000016	$1\pi \rightarrow 5\pi$ (R)
$^2\Sigma^+$	21.28	0.00045	$5\sigma \rightarrow 5\pi, 4\sigma \rightarrow 5\pi$ (R)
$^2\Sigma^-$	18.37	0.013	$1\pi \rightarrow 9\sigma, 1\pi \rightarrow 10\sigma$ (R)
$^2\Sigma^-$	18.24	0.00073	$1\pi \rightarrow 9\sigma, 1\pi \rightarrow 10\sigma, 5\sigma \rightarrow 3\pi$ (R)
$^2\Delta$	17.70	0.032	$5\sigma \rightarrow 3\pi(R), 1\pi5\sigma \rightarrow 2\pi^2$ (NR)
N $3p\ ^4D^0$ + O ^3P			
$^2\Pi$	17.92	0.00020	$5\sigma^2 \rightarrow 2\pi^2, 4\sigma5\sigma \rightarrow 2\pi^2$ (NR)
$^2\Pi$	17.60	0.011	$1\pi \rightarrow 6\pi, 5\sigma \rightarrow 7\sigma$ (R)
$^2\Pi$	17.63	0.016	$1\pi \rightarrow 6\pi, 5\sigma \rightarrow 7\sigma$ (R)
$^2\Sigma^+$	20.77	0.029	$5\sigma \rightarrow 6\pi$ (R) + continuum
$^2\Sigma^+$	20.26	0.00019	$5\sigma \rightarrow 4\pi, 4\sigma \rightarrow 4\pi$ (R)
$^2\Sigma^-$	18.24	0.0013	$1\pi \rightarrow 9\sigma, 1\pi \rightarrow 10\sigma, 5\sigma \rightarrow 3\pi$ (R)
$^2\Delta$	17.55	0.0042	$5\sigma \rightarrow 3\pi$ (R), $1\pi5\sigma \rightarrow 2\pi^2$ (NR)
$^2\Delta$	17.39	0.0000032	$1\pi \rightarrow 9\sigma, 1\pi \rightarrow 10\sigma$ (R)
O $3p^3P$ + N ^4S			
$^2\Pi$	17.40	0.0013	$1\pi \rightarrow 4\pi, 1\pi \rightarrow 5\pi$ (R)
$^2\Sigma^+$	18.35	0.015	$5\sigma \rightarrow 3\pi, 1\pi \rightarrow 1\delta$ (R)
O $3p^5P$ + N ^4S			
$^2\Pi$	17.09	0.0011	$1\pi \rightarrow 3\pi, 1\pi \rightarrow 4\pi$ (R)
$^2\Sigma^+$	17.92	0.021	$4\sigma \rightarrow 2\pi, 1\pi5\sigma \rightarrow 2\pi^2$ (NR)

The initial state for the electric dipole strength is the $^2\Pi$ ground state. In the last column showing the dominant excitations, (R) and (NR) indicate Rydberg and non-Rydberg states, respectively.

vibrational levels, and they tend to have a potential maximum at some (large) R-value. Now, if the molecule is excited to a vibrational level closely below the potential maximum, it may dissociate by tunnelling through the barrier. From Figs. 4 and 5 we see that there are two groups of excited states, one with potential minima in the region 17.5–18 eV, and another with minima around 20.5–21.5 eV. Thus, with reference to the tunnelling mechanism discussed above, we have a reasonable explanation for the dominant structures shown in Fig. 3. For neutral dissociation to the N $3p^4D^0$ as well as the N $3p^4P^0$ limits the experimental results of Fig. 3(a) show a prominent and rather narrow peak at about 18.5 eV, in accordance with the lower group of states of Figs. 4 and 5, respectively. A somewhat broader structure around 21.5 eV in both cases agrees quite well with the higher states of Figs. 4 and 5.

In a similar manner the potential curves of Fig. 6 may explain the observed structures shown in Fig. 3(d) related to neutral dissociation to the O $3p^5P$ and O $3p^3P$ limits. The lower $^2\Pi$ curves of Fig. 6 may give rise to the structures around 18 eV of Fig. 3(d). For both dissociation limits there is in addition a higher $^2\Sigma^+$ curve that tend to have a higher potential maximum, and which might explain the observed structures at about 20.5 eV (prominent for the O $3p^5P$ limit).

In addition to tunnelling there is also the possibility of dissociation caused by predissociation of the doublet precursor states. Probable predissociating agents are a series of molecular quartet states that correlate with the relevant dissociation limits. The locations and shapes of the quartet state potential curves have so far not been investigated in any detail, but they seem to fall in the relevant energy region. Predissociations may in particular

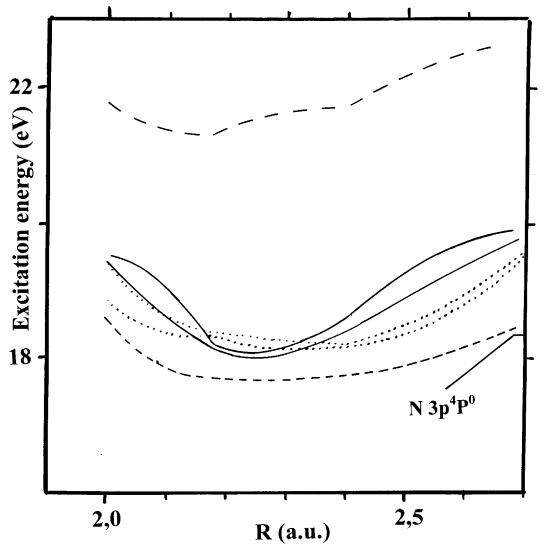

Fig. 4. Potential curves for doublet states in NO which correlate with the N $3p^4P^0$ + O ^3P (ground state) dissociation limit. Solid, $^2\Pi$ states; long dashes, $^2\Sigma^+$ states; dots, $^2\Sigma^-$ state; and short dashes, $^2\Delta$ state.

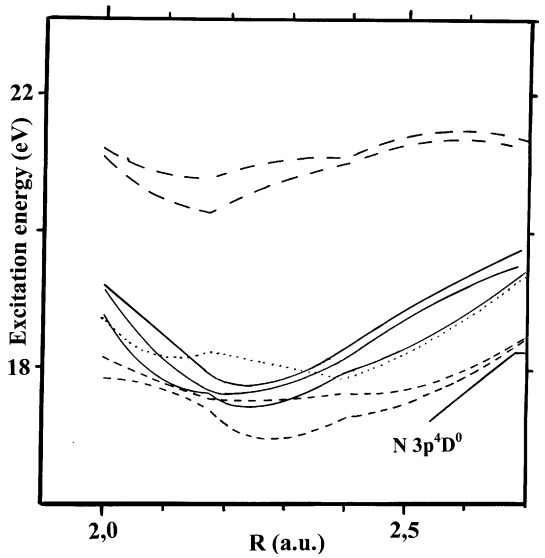

Fig. 5. Potential curves for doublet states in NO which correlate with the N $3p^4D^0$ + O ^3P (ground state) dissociation limit. Solid, $^2\Pi$ states; long dashes, $^2\Sigma^+$ state; dots, $^2\Sigma^-$ states; and short dashes, $^2\Delta$ state.

explain several minor structures in the observed results. Ab initio calculations related to the several other higher dissociation levels observed in the present work, have so far not been carried out due to the increasing density and complexity of molecular states at higher energies.

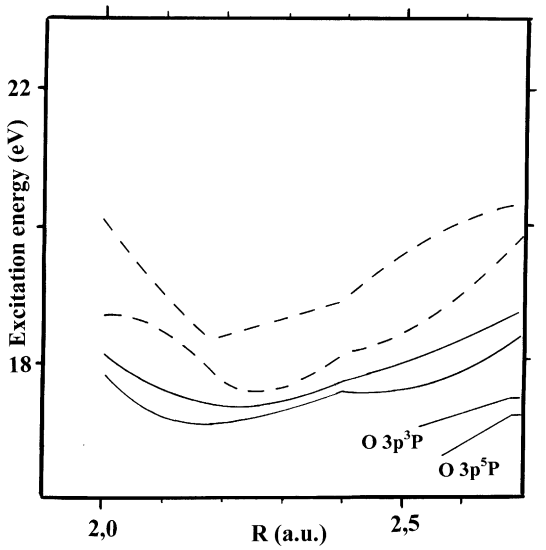

Fig. 6. Potential curves for doublet states in NO which correlate with the O $3p^3P$ – and O $3p^5P$ + N^4S (ground state), O $3p^3P$ limit: upper solid ($^2\Pi$) and upper dashes ($^2\Sigma^+$), O $3p^5P$ limit: lower solid ($^2\Pi$) and lower dashes ($^2\Sigma^+$).

Estimates of the accuracies of the present ab initio excitation energies are certainly of interest. The comparisons of experimental and theoretical results above tend to indicate accuracies of about 0.5 eV. In the next section we will also see that excitation energies for members of the *R*(c) Rydberg series are predicted within a few tenths of an eV. Finally, vertical excitation energies were also computed for a series of low-lying states in NO, e.g., the $A^2\Sigma^+$, $D^2\Sigma^+$, $E^2\Sigma^+$, $C^2\Pi$, $B^2\Pi$, $b^4\Sigma^-$ and $a^4\Pi$ states. Compared with experimental vertical excitation energies [17] we found that our computed ones were all systematically shifted upwards by about 0.8 eV. Such a systematic shift is not unexpected from the present type of variational method (limited CI), which tends to favor the ground state (lower energy) as the molecular orbitals used for the CI-expansions are optimized for the ground state. Consequently, all our computed excitation energies were "calibrated" by subtracting an amount of 0.8 eV before comparison with experiment or presentation in Table 1.

The use of finite basis sets is another source of inaccuracies. In the present work we made an effort to include as many diffuse atomic orbitals as numerically feasible to account for the Rydberg character of the excited NO-states. Thus, we have no real account of the sensitivity of our results to the basis sets, but we believe that the major source of inaccuracies lies in the limited CI-expansions.

5. Molecular emission induced by 21.2–21.4 eV photons

Three fairly weak lines at $\lambda = 716$, 718 and 722 nm occur in the observed emission spectrum from photon excited NO, but only at excitation wavelengths 580 and 585 Å ($h\nu = 21.38$ and 21.19 eV). There are no known atomic emission lines neither in NI or OI at these wavelengths and they should therefore be of molecular origin. Fig. 7 shows the first dissociation limits in NO^+ and the potential curves in NO^+ having these limits are indicated in the figure (from [18]). To get molecular emission in NO^+, one obviously has to excite one of the states having the second limit since only two NO^+ states have the first limit and a–X emission is forbidden. Since the energy of the second limit (relative to the NO ground state) is 21.03 eV, this means that NO^+ emission can occur following autoionization of the first NO Rydberg levels above this limit. As follows from [8] these levels are R(c), $v = 0$ 6sσ at 21.18 eV, 7sσ at 21.35 eV, 5dπ at 21.14 eV and 6dπ at 21.31 eV and photon excitation of NO with this energy range could lead to autoionization to the continuum of states having the second limit. After relaxation these states may then decay by fluorescence to a lower NO^+ state in accordance with our observations. With increasing $h\nu$, higher levels of the R(c) series are excited, but the populations rapidly drop up to the ionization limit at 21.73 eV. This readily explains the very narrow excitation range of the $\lambda = 716$, 718 and 722 nm lines. In view of the sparse spectroscopic data on NO^+, it is difficult to identify the involved states of these emission lines. Possible candidates would be the $A^1\Pi$–$A'^1\Sigma^-$ or the $A^1\Pi$–$W^1\Delta$ system. The rotational structures of these bands are so narrow that they appear as "single lines" at the present experimental resolution.

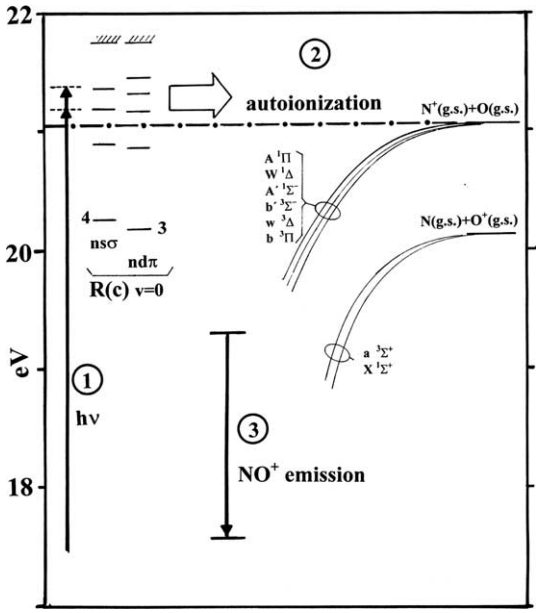

Fig. 7. Explanation of the origin of molecular emission bands at $\lambda = 716$, 718 and 722 nm occurring in the photon excitation range $h\nu = 21.2$–21.4 eV. In this energy range the excitation **1** may populate Rydberg levels R(c) of various symmetries which are just above the second dissociation limit of NO^+. These Rydberg levels may decay **2** by autoionization to the continuum of NO^+ states like the $A\ ^1\Pi$ state, which subsequently decays **3** by fluorescence to another, lower lying NO^+ state, for instance the $A'\ ^1\Sigma^-$ or the $W\ ^1\Delta$ state.

The present ab initio calculations give some interesting indications regarding the NO precursor states for these emission lines. There are two $^2\Pi$ states derived from the excited molecular configuration $4\sigma 5\sigma^2\pi^4 2\pi 7\sigma$, with computed excitation energies at 21.17 and 21.58 eV, respectively, and with particularly large electric dipole strengths, i.e., 0.020 and 0.055 a.u., respectively. The excited 7σ orbital is a diffuse orbital of Rydberg character, which means that the two $^2\Pi$ states are part of the R(c) Rydberg series, as expected. The current $^2\Pi$ states have strong interactions with continuum states associated with the following three NO^+ configurations: $4\sigma^2 5\sigma^2 1\pi^4$, $4\sigma^2 5\sigma 1\pi^4 2\pi$ and $4\sigma^2 5\sigma^2 1\pi^3 2\pi$. Thus, several excited NO^+ states derived from the last two of these three configurations may be the end products of the autoionization process,

and thereby also initial states for the present emission lines.

Two other interesting candidates are a $^2\Sigma^+$ state and a $^2\Delta$ state with computed excitation energies at 20.77 and 22.00 eV, respectively, also with large electric dipole strengths (0.031 and 0.010 a.u., respectively). These two states are ascribed to a mixture of the two configurations $4\sigma5\sigma^21\pi^42\pi6\pi$ and $4\sigma^25\sigma1\pi^42\pi6\pi$, and are thereby also part of the R(c) Rydberg series, as the 6π orbital is another orbital of Rydberg character. In this case there is strong interaction with the continuum from the $4\sigma^25\sigma^21\pi^32\pi$ NO^+ configuration, with a subsequent possibility of autoionization to the NO^+ excited states derived from this configuration.

Ab initio calculations based on a finite set of atomic orbitals can obviously not reproduce an infinite set of Rydberg orbitals. It is, however, believed that the present inclusion of a rather extensive set of diffuse atomic orbitals will lead to reasonable approximations to a few of the lowest Rydberg orbitals of σ, π and δ symmetry. However, working with molecular orbitals there is no explicit specification of the atomic angular momentum quantum number ℓ.

6. Conclusions

We have studied the near-infrared fluorescence from nitric oxide excited by 17.2–25.8 eV photons. The intensities of 13 resolved multiplets of NI and OI are studied as a function of the excitation energy. Since the structure of these excitation functions showed a poor coincidence with known NO Rydberg levels in the same energy region, ab initio calculations were performed in order to make an attempt at identifying the actual NO states responsible for the observed neutral dissociation. The calculations suggest that there are a number of "new" NO states with symmetries $^2\Sigma^+$, $^2\Sigma^-$, $^2\Pi$ and $^2\Delta$ in the energy range 17.1–21.3 eV which are responsible for the observed neutral dissociation of NO. Three "new" molecular NO^+ emission bands are observed in a narrow excitation range (21.1–21.4 eV) and the calculations indicate that they are primarily formed in autoionization of two NO $^2\Pi$ states derived from the configuration $4\sigma5\sigma^21\pi^42\pi7\sigma$, or a $^2\Sigma^+$ and a $^2\Delta$ state derived from a mixing of $4\sigma5\sigma^21\pi^42\pi6\pi$ and $4\sigma^25\sigma1\pi^42\pi6\pi$.

References

[1] P. Erman, E. Rachlew-Källne, S.L. Sorensen, Zeitschr. Phys. D 30 (1994) 315.
[2] A. Ehresmann, S. Machida, M. Ukai, K. Kameta, M. Kitajima, N. Kouchi, Y. Hatano, K. Ito, T. Hayaiski, J. Phys. B 28 (1995) 5283.
[3] J. Álvarez Ruiz, P. Erman, E. Rachlew-Källne, J. Rius i Riu, M. Stankiewicz, L. Veseth, J. Phys. B 35 (2002) 2975.
[4] P. Erman, A. Karawajczyk, E. Rachlew-Källne, S.L. Sorensen, C. Strömholm, M. Kirm, J. Phys. B 26 (1993) 4483.
[5] P. Erman, A. Karawajczyk, E. Rachlew-Källne, J. Rius i Riu, M. Stankiewicz, K. Yoshiki Franzén, L. Veseth, Phys. Rev. A 60 (1999) 426.
[6] M. Ukai, S. Machida, K. Kameta, M. Kitajima, N. Kouchi, Y. Hatano, K. Ito, Phys. Rev. Lett. 74 (1995) 239.
[7] A. Karawajczyk, P. Erman, E. Rachlew-Källne, J. Rius i Riu, M. Stankiewicz, K. Yoshiki Franzén, L. Veseth, Phys. Rev. A 61 (2000) 032718.
[8] P. Erman, A. Karawajczyk, E. Rachlew-Källne, C. Strömholm, J. Chem. Phys. 102 (1995) 3064.
[9] A. Ehresmann, H. Liebel, M. Von Kröger, H. Schmoranzer, J. Phys. B 34 (2001) 3119.
[10] P. Erman, A. Karawajczyk, U. Köble, E. Rachlew-Källne, K. Yoshiki Franzén, L. Veseth, Phys. Rev. Lett. 76 (1996) 4136.
[11] R.G. Parr, W. Yang, Density-Functional Theory of Atoms and Molecules, Oxford University Press, Oxford, 1989.
[12] L. Veseth, J. Chem. Phys. 114 (2001) 8789.
[13] S. Ivanov, S. Hirata, R.J. Bartlett, Phys. Rev. Lett. 83 (1999) 5455.
[14] A. Görling, Phys. Rev. Lett. 83 (1999) 5459.
[15] P.E. Cade, W.M. Huo, Atom. Data Nucl. Data 15 (1975) 1.
[16] L.D. Landau, E.M. Lifshitz, Quantum Mechanics, Pergamon Press, Oxford, 1962.
[17] F.R. Gilmore, J. Quant. Spectrosc. Radiat. Transfer 5 (1965) 369.
[18] D.L. Albritton, A.L. Schmeltekopf, R.N. Zare, J. Chem. Phys. 71 (1979) 3271.